JOURNAL OF GEOPHYSICAL RESEARCH, VOL. 98, NO. D12, PAGES 22,987–22,994, DECEMBER 20, 1993

Stratospheric Aerosol Optical Depths, 1850–1990

MAKIKO SATO AND JAMES E. HANSEN

NASA Goddard Institute for Space Studies, New York

M. PATRICK MCCORMICK

NASA Langley Research Center, Hampton, Virginia

JAMES B. POLLACK

NASA Ames Research Center, Moffett Field, California

A global stratospheric aerosol database employed for climate simulations is described. For the period 1883–1990, aerosol optical depths are estimated from optical extinction data, whose quality increases with time over that period. For the period 1850–1882, aerosol optical depths are more crudely estimated from volcanological evidence for the volume of ejecta from major known volcanoes. The data set is available over Internet.

1. INTRODUCTION

Stratospheric aerosol amount is highly variable as a result of sporadic volcanic eruptions [*Lamb*, 1970; *Mitchell*, 1970; *Pollack et al.*, 1976*a*; *Robock*, 1981; *McCormick and Trepte*, 1987]. The aerosols affect the Earth's radiation balance, principally by reflecting sunlight to space and, secondarily, by absorbing upwelling terrestrial thermal radiation [*Coakley and Grams*, 1976; *Harshvardhan and Cess*, 1976; *Pollack et al.*, 1976*b*; *Hansen et al.*, 1980; *Lacis et al.*, 1992], and thus they are a potentially significant climate forcing on timescales of years, decades, and longer periods. Theoretical and empirical evidence, although somewhat mixed, on balance suggests that large volcanoes do influence global climate measurably [*Mass and Schneider*, 1977; *Hansen et al.*, 1978; *Stommel and Stommel*, 1983; *Kelly and Sear*, 1984; *Stothers*, 1984; *Angell and Korshover*, 1985; *Rampino et al.*, 1988; *Self and Rampino*, 1988; *Mass and Portman*, 1989; *Robock*, 1991; *Dutton and Christy*, 1992; *Hansen et al.*, 1993]. Climate forcing by stratospheric aerosols at times may exceed that of anthropogenic greenhouse gases [*Hansen and Lacis*, 1990], but it is not so accurately known, and thus its uncertainty represents an obstacle to quantitative analysis of past climate change.

The principal parameter affecting stratospheric aerosol climate forcing is the optical depth of the aerosol layer [*Lacis et al.*, 1992]. We describe here a data set of stratospheric aerosol optical depth for the period from 1850 to the present, which we employed in a set of global climate simulations for that period [*Hansen et al.*, 1993]. The data set may be useful to other climate researchers, at least for the sake of comparison. We describe the sources of our data and the reasons for choices among alternative sources. We would welcome information on any observations with potential for improving this data set. The data set and future revisions of it are available from the authors via Internet with data access procedures described below.

Paper number 93JD02553.

2. DATA SOURCES

We divide our discussion of stratospheric aerosol data sources into four periods (Figure 1), which have successively improved data quality. In period 1 (1850–1882) we have only very crude estimates of aerosol optical thickness based on the volume of ejecta from major known volcanoes, supported by qualitative reports of atmospheric optical phenomena. Period 2 (1883–1959) has measurements of solar extinction, but during the time of principal volcanic activity (1883–1915) the data are confined to middle-latitude northern hemisphere observatories. Period 3 (1960–1978) has more widespread measurements of solar and stellar extinction, lunar eclipses, and some in situ sampling of aerosol properties. Period 4 (1979–1990) adds precise widespread data from satellite measurements.

Period 1 (1850–1882). Estimates of stratospheric aerosol optical thickness ideally should be based on measurements of optical extinction. Since we are unaware of such data for the period 1850–1882, we are forced to obtain a rough estimate from volcanologic evidence. Any estimate based on such evidence is highly problematical, because aerosol optical depth depends mainly on the amount of sulfur emitted rather than the size of the eruption. Fortunately, errors in aerosol optical depth during this period have relatively little effect on simulated climate in recent and future decades.

A widely used stratospheric aerosol index is the "dust veil index" of *Lamb* [1970]. Lamb's index is based in part on observed midlatitude temperature anomalies, a circularity which makes it not directly useful for our purposes. However, *Mitchell* [1970] used Lamb's estimates of the volume of ejecta from known volcanoes (the original source being primarily *Sapper* [1927]) to construct an index for the period 1850–1970 intended to be proportional to "stratospheric aerosol loading." Some justification for using Mitchell's index for the period 1850–1882 is provided by the qualitative resemblance of this index for the period 1883–1970 to the aerosol optical depths estimated below on the basis of atmospheric extinction measurements. In many instances, Mitchell's index differs from what would be obtained from

the more recent compilations of *Simkin et al.* [1981] and *Newhall and Self* [1982]. We use Mitchell's index which is reasonably consistent with measured aerosol optical depths in the twentieth century, and we emphasize that Mitchell's index only affects our optical depths in the period 1850–1882. Table 1 lists Mitchell's "severity" classification for volcanoes since 1850 as well as the volcanic explosivity index (VEI) of *Newhall and Self* [1982] for the same volcanoes. Recent additions to VEI were obtained from S. Self, private communication, 1993.

In the period 1850–1882 the volcanoes contributing most to Mitchell's stratospheric loading (Table 1) are Cotopaxi (Ecuador, 1°S, 1855), Awu (Celebes, 4°N, 1856), Makjan (Molucca Islands, 0.3°N, 1861), and Askja (Iceland, 65°N, 1875). Evidence supporting the radiative significance of stratospheric aerosols following these eruptions is provided by unusually colored sunsets and other optical phenomena observed in midlatitudes of the northern hemisphere [*Lamb*, 1970]. We obtained a scale factor to convert Mitchell's stratospheric mass loading (his Figure 3) to an optical depth (0.0025 per million metric tons) by equating the integral of the aerosol loading over the period 1883–1970 to the integral of the optical depth which we estimate below for that period; the same scale factor was obtained from comparison of the aerosol loading and optical depth after the largest volcano, Krakatau.

We must specify the global distribution of aerosols for three-dimensional climate simulations. *Lamb* [1970] discussed the expected geographical distribution of stratospheric aerosols as a function of the latitude of the volcanic eruption, based on the climatological nature of stratospheric winds. Essentially, he assumed that aerosols from low-latitude eruptions would spread uniformly over the globe, while aerosols from higher-latitude volcanoes would tend to be more confined to the zone of the eruption and poleward within that hemisphere. But data from volcanoes in the past few decades reveal marked exceptions to Lamb's expectations, especially the 1963 Agung (8°S) eruption, which produced 4 times more optical depth in the southern hemisphere than in the northern hemisphere [*Dyer and Hicks*, 1968]. Agung may have been an extreme case, in which the atmospheric winds at the time of the eruption carried the material very efficiently into the southern hemisphere, but other recent eruptions confirm the difficulty of specifying latitudinal distributions. El Chichon, at 17°N latitude, caused an aerosol optical depth twice as large in the northern hemisphere as in the southern hemisphere, but Pinatubo, at about the same latitude (15°N), resulted in approximately as much optical depth in the southern hemisphere as in the northern hemisphere. These examples illustrate the magnitude of errors that may occur with simple assumptions about the global distribution of aerosols. Nevertheless, in the absence of optical depth measurements at multiple locations, we must make some assumption about the global distribution of aerosols. Based on the latitudes of the eruptions in the period 1850–1882 and the lack of other data, we assume that the aerosols were uniformly distributed over the globe in that period, except the aerosols following Askja, which we confine to latitudes 30° to 90°N.

Period 2 (1883–1959). For this period there are measurements of atmospheric optical extinction, mainly from middle latitudes of the northern hemisphere. The most useful data are several long series (1883–1923) of measurements of solar

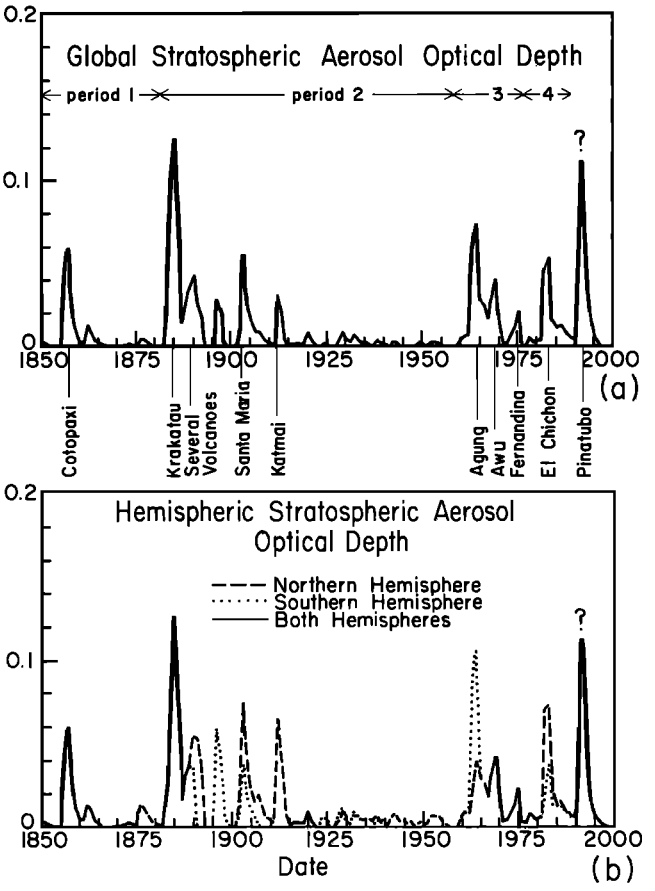

Fig. 1. Estimated stratospheric aerosol optical depth at $\lambda = 0.55$ μm: (*a*) global mean and (*b*) hemispheric means.

irradiance compiled by *Kimball* [1924]. The data were acquired at several stations between 31° and 56°N, the longest single record being at Pavlovsk (56°N) from 1892 to 1913. During the important period 1883–1892, data were obtained at only one station, Montpelier (44°N). In addition to the restricted geographical coverage, most of the data were acquired at a single solar zenith angle. Thus the aerosol optical depth must be inferred from temporal change of solar intensity under the assumption of constant solar irradiance. It is also assumed that there is no change of instrumental sensitivity with time and that a zero optical depth can be defined for reference years removed from the times of significant volcanic influence.

Both *Dyer* [1974] and *Toon* [1975] use Kimball's data, obtaining somewhat different results in the period 1883–1892 because of differing assumptions about the zero point of optical depth in the reference years. Dyer specifies 1887 and 1889 as reference years with zero optical depth. This seems likely to underestimate the stratospheric optical depth, especially considering the known moderate eruptions in 1886 and 1888 (Table 1). Toon's zero point is lower, resulting in positive definite optical depths at seasonal temporal resolutions. This may overestimate the optical depth, because some of the short-term variability is probably noise, which is apparent in the observations at all times. We choose an intermediate zero point, 0.02 lower than that of Dyer.

In the absence of southern hemisphere measurements we estimate southern hemisphere optical depths based on the

TABLE 1. Volcanoes in the Period 1850–1991 of Severity Class 2 or Higher

Date	Volcano	Latitude, Longitude	Severity	VEI
1854, Feb.	Sheveluch, Kamchatka	57°N, 162°E	...	5
1855–1856	Cotopaxi, Ecuador	1°S, 78°W	1.5	...
1856, Feb.	Awu, Celebes	4°N, 125°E	2	...
1861, Dec.	Makjan, Molucca Islands	0°N, 127°E	2	4
1875, March	Askja, Iceland	65°N, 17°W	2	5
1883, Aug.	Krakatau, Indonesia	6°S, 105°E	1	6
1886, June	Tarawera, New Zealand	38°S, 177°E	2	5
1888, March	Ritter Island, Bismarck Archipelago	6°S, 148°E	2	...
1888, July	Bandai San, Japan	38°N, 140°E	2	4
1892, June	Awu, Celebes	4°N, 125°E	2	...
1902, May	Mont Pelée, Martinique	15°N, 61°W	2	4
1902, May	Soufrière, St. Vincent	13°N, 61°W	2	4
1902–1904	Santa Maria, Guatemala	15°N, 92°W	1.33	5–6
1907, March	Shtyubelya, Kamchatka	52°N, 158°E	2	5
1912, June	Katmai, Alaska	58°N, 155°W	2	6
1932, April	Quizapu, Cerro Azul	36°S, 71°W	3	5
1947, March	Hekla, Iceland	64°N, 20°W	2	4
1953, July	Mount Spurr, Alaska	61°N, 152°W	2	4
1956, March	Bezymyannaya, Kamchatka	56°N, 161°E	2	5
1963, March	Gunung Agung, Bali	8°S, 116°E	1.5	4
1966, Aug.	Awu, Celebes	4°N, 125°E	2	4
1968, June	Fernandina Island, Galapagos	0°S, 92°W	2	4
1980, May	St. Helens, United States	46°N, 122°W	...	5
1982, April	El Chichon, Mexico	17°N, 93°W	...	5
1991, June	Pinatubo, Philippines	15°N, 120°E	...	5
1991, Aug.	Hudson, Chile	46°S, 73°W	...	5

The severity numbers 1, 2, 3 of *Mitchell* [1970] are intended by the author to represent volumes of ejecta 1–10, 0.1–1, 0.01–0.1 km^3, respectively. Volcanic explosivity index (VEI) numbers 6, 5, 4 of *Newhall and Self* [1982] are intended by the authors to represent volumes of ejecta 10–100, 1–10, 0.1–1 km^3, respectively.

latitudes (Table 1) of the known principal volcanoes. The eruption believed to be the largest in period 2, Krakatau (Indonesia, 6°S, 1883), was located in the near-equatorial zone; hence we used the same optical depth in the southern hemisphere as measured in the northern hemisphere. Some justification for this assumption is provided by similar sulfur amounts in Arctic and Antarctic ice cores for the period following Krakatau [*Hammer et al.*, 1980; *Thompson and Mosley-Thompson*, 1981]. The period 1886–1888 contained three of Mitchell's "severity 2" volcanoes. Because of the symmetry of these volcanoes about the equator (Table 1) we assume that the optical depth in the southern hemisphere was also the same as in the northern hemisphere during 1886–1889.

In the period 1890–1892, for which *Dyer* [1974] assumes the measured optical depth originated from Bogoslov (54°N), we take the optical depth at 0°–30°N as half of that for 30°–90°N and zero optical depth in the southern hemisphere. In the period 1896–1898, assumed by *Dyer* [1974] to be affected by Thompson Island (54°S), we use an optical depth the same as during 1890–1892 but placed in the southern hemisphere. In the period 1902–1906, presumably affected by the Mont Pelée (15°N), Soufrière (13°N), and Santa Maria (15°N) eruptions, we take the optical depth in the southern hemisphere to be half of that measured in the northern hemisphere. In the period 1907–1911, presumably affected by Shtyubelya (52°N), we used the optical depth measured at Pavlovsk (56°N) for 30°–90°N, with zero optical depth elsewhere (little, if any, optical depth perturbation was measured at Simla (31°N)]. In the period 1912–1915, affected by Katmai (58°N), we used the optical depth measured at Pavlovsk (56°N) for the region 30°–90°N and the optical depth measured at Simla (31°N) for latitudes 0°–30°N, with zero optical depth in the southern hemisphere.

Stratospheric aerosol optical depths were apparently very small in the period 1920–1959. *Pollack et al.* [1976*a*, *b*], for example, assume zero stratospheric aerosol optical depth in that period, citing lack of any evidence for substantial volcanoes in the solar extinction measurements during that period. *Mitchell* [1970] lists only three volcanoes of severity 2 during that period: Hekla (Iceland, 64°N, 1947), Mount Spurr (Alaska, 61°N, 1953), and Bezymyannaya (Kamchatka, 56°N, 1956) and no volcanoes of greater magnitude. Various studies of atmospheric transmission for the period 1920–1959 contain indications of only small opacities; for example, the long 1909–1979 atmospheric transmission record at Davos, Switzerland (Hoyt and Frohlich, 1983), shows large reductions only in 1912 (Katmai) and 1963 (Agung), with smaller reductions in the 1950s. Although the optical depths in the period 1920–1959 are small, we estimate the largest contributions from extinction data published by *Hoyt* [1978, 1979*a*, *b*] and *Hoyt and Frohlich* [1983]. These data yield optical depths approaching 0.01 in both hemispheres for periods about 1929 and 1932 and about 0.006 (annual mean) in the northern hemisphere in the early 1950s, as shown in Figure 1 and Table 2. The eruptions which were probably responsible for these observed optical depths are included in Table 1.

Period 3 (1960–1978). During this period, measurements of atmospheric extinction were obtained at sites in both hemispheres. We rely especially on the astronomical observations before and after the 1963 Agung eruption summa-

TABLE 2. Estimated Annual Stratospheric Aerosol Optical Depths (Multiplied by 1000) at $\lambda = 0.55\ \mu m$

		NH		SH				NH		SH				NH		SH	
Year	Global	90°–30°	30°–0°	0°–30°	30°–90°	Year	Global	90°–30°	30°–0°	0°–30°	30°–90°	Year	Global	90°–30°	30°–0°	0°–30°	30°–90°
1850	3	3	3	3	3	1900	0	0	0	0	0	1950	1	0	0	3	3
1851	2	2	2	2	2	1901	0	0	0	0	0	1951	1	2	2	0	0
1852	1	1	1	1	1	1902	12	16	16	8	8	1952	3	6	6	0	0
1853	0	0	0	0	0	1903	55	74	74	37	37	1953	3	6	6	0	0
1854	0	0	0	0	0	1904	27	36	36	18	18	1954	3	6	6	0	0
1855	0	0	0	0	0	1905	15	20	20	10	10	1955	1	3	3	0	0
1856	39	39	39	39	39	1906	10	13	13	6	6	1956	0	1	1	0	0
1857	60	60	60	60	60	1907	10	39	0	0	0	1957	0	0	0	0	0
1858	26	26	26	26	26	1908	6	24	0	0	0	1958	0	0	0	0	0
1859	11	11	11	11	11	1909	3	10	0	0	0	1959	0	0	0	0	0
1860	4	4	4	4	4	1910	2	9	0	0	0	1960	5	5	5	5	5
1861	3	3	3	3	3	1911	1	4	0	0	0	1961	7	2	14	10	2
1862	14	14	14	14	14	1912	32	98	30	0	0	1962	8	3	8	17	4
1863	10	10	10	10	10	1913	21	50	35	0	0	1963	53	10	33	92	75
1864	4	4	4	4	4	1914	4	0	16	0	0	1964	72	25	53	132	76
1865	2	2	2	2	2	1915	1	0	2	0	0	1965	27	31	25	24	30
1866	1	1	1	1	1	1916	2	2	2	2	2	1966	25	25	25	25	25
1867	0	0	0	0	0	1917	2	2	2	2	2	1967	17	17	17	17	17
1868	0	0	0	0	0	1918	2	2	2	2	2	1968	32	32	32	32	32
1869	0	0	0	0	0	1919	2	2	2	2	2	1969	41	41	41	41	41
1870	0	0	0	0	0	1920	9	9	9	9	9	1970	19	19	19	19	19
1871	0	0	0	0	0	1921	3	3	3	3	3	1971	2	2	2	2	2
1872	1	1	1	1	1	1922	0	0	0	0	0	1972	3	3	3	3	3
1873	3	3	3	3	3	1923	0	0	0	0	0	1973	8	8	8	8	8
1874	2	2	2	2	2	1924	3	0	0	6	6	1974	13	13	13	13	13
1875	0	1	0	0	0	1925	2	0	0	4	4	1975	22	22	22	22	22
1876	6	25	0	0	0	1926	1	2	2	0	0	1976	2	2	2	2	2
1877	5	21	0	0	0	1927	0	0	0	0	0	1977	1	1	1	1	1
1878	3	12	0	0	0	1928	5	2	2	8	8	1978	7	7	7	7	7
1879	2	8	0	0	0	1929	10	8	8	11	11	1979	4	4	4	4	4
1880	1	4	0	0	0	1930	5	6	6	5	5	1980	4	5	5	3	3
1881	0	2	0	0	0	1931	3	6	6	0	0	1981	5	5	5	4	4
1882	0	1	0	0	0	1932	8	6	6	10	10	1982	46	33	105	29	14
1883	21	21	21	21	21	1933	6	5	5	7	7	1983	55	89	59	35	37
1884	81	81	81	81	81	1934	3	3	3	3	3	1984	16	23	18	10	14
1885	125	125	125	125	125	1935	4	4	4	3	3	1985	13	16	10	10	14
1886	78	78	78	78	78	1936	2	4	4	0	0	1986	13	13	16	13	11
1887	16	16	16	16	16	1937	2	3	3	0	0	1987	10	13	9	8	11
1888	31	31	31	31	31	1938	5	6	6	3	3	1988	7	8	5	6	10
1889	37	37	37	37	37	1939	3	2	2	4	4	1989	6	6	4	5	9
1890	43	60	47	33	33	1940	2	1	1	3	3	1990	6	7	4	5	8
1891	26	70	35	0	0	1941	0	1	1	0	0						
1892	18	47	23	0	0	1942	4	8	8	0	0						
1893	0	0	0	0	0	1943	3	7	7	0	0						
1894	0	0	0	0	0	1944	1	3	3	0	0						
1895	0	0	0	0	0	1945	2	3	3	0	0						
1896	29	0	0	39	77	1946	1	1	1	0	0						
1897	22	0	0	30	59	1947	1	3	3	0	0						
1898	3	0	0	4	7	1948	0	0	0	0	0						
1899	0	0	0	0	0	1949	3	2	2	3	3						

The four equal-area zones are 90°–30°N, 30°N-equator, equator-30°S, and 30°–90°S, respectively.

rized by *Dyer and Hicks* [1968]. Also coarser information is provided by analysis of lunar eclipses throughout this period by *Keen* [1983]. The eclipse data are in reasonably good agreement with the other astronomical extinction data in instances where both are available.

Total lunar eclipses, which occur on average about once per year, provide the opportunity to measure the brightness of sunlight refracted and scattered by the Earth's atmosphere into the Earth's geometrical shadow. Following large volcanic eruptions, stratospheric aerosols have a dominant influence on the brightness in the Earth's shadow [*Link*, 1963; *Hansen and Matsushima*, 1966]. The lunar brightness is dependent on aerosol amount at all latitudes, but the latitudes are unequally weighted, depending upon the Moon's position in the Earth's shadow. Because of this characteristic and the infrequent occurrence of eclipses, this technique provides only a coarse, though useful, measure of aerosol optical depth. *Keen* [1983] analyzed 21 eclipses between 1960 and 1982, finding maximum visible optical depths in December 1963 (0.13), December 1982 (0.12), and October 1968 (0.06), which were after the Agung, El Chichon, and Fernandina eruptions, respectively. Figure 2 of *Keen* [1983] gives the optical depth for the period 1960–1982 based on the 21 eclipses.

Dyer and Hicks [1968] give aerosol optical depth for nine latitude bands for the period 1961–1965. We interpolate these data to our general circulation model (GCM) grid for climate simulations; the resulting optical depth as a function of latitude and time is shown in Figure 2*a*. Dyer and Hicks note that their sampling is very poor in the southern hemisphere, especially at low latitudes. Thus the nature of the double maximum of the optical depth, with a peak in mid-1964, should not be taken too seriously, but it is clear that there were very large optical depths in the southern hemisphere from mid-1963 through 1964. Integrated over the globe the maximum annual mean optical depth after the Agung eruption is 0.08 in 1964 (Figure 1). This is consistent with the eclipse value 0.13 of *Keen* [1983] which refers to a day in December 1963 and weights the southern hemisphere more than the northern hemisphere. Also *Lockwood and Thompson* [1986], with observations at Cerro Tololo (30°S) and Lowell Observatory (35°N), found values consistent with those of Dyer and Hicks, including the four to one ratio of

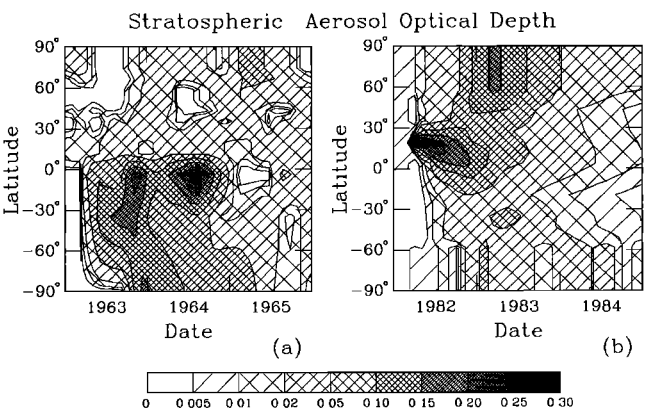

Fig. 2. Estimated stratospheric aerosol optical depth at $\lambda = 0.55$ μm as a function of latitude and time: (*a*) period after Agung and (*b*) period after El Chichon.

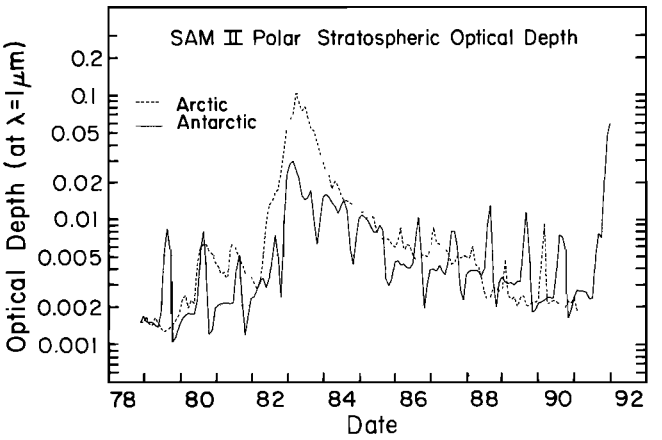

Fig. 3. Monthly mean polar stratospheric aerosol optical depths at $\lambda = 1$ μm measured by SAM II; values in early 1983 are corrected for instrument saturation.

southern hemisphere and northern hemisphere optical depths.

For the period 1966–1978 we use the optical depths of *Keen* [1983] based on lunar eclipse data, interpolated linearly between the dates of observations. The optical depths are small during this period, the largest contribution being from Fernandina (Galapagos, 0.4°S, 1968). Because of the generally small values and the equatorial location of Fernandina, we take the aerosols as uniformly distributed in the period 1966–1978.

Period 4 (1979–1990). Extensive satellite data begin with stratospheric aerosol monitor (SAM) II on the Nimbus 7 satellite launched in late 1978 [*McCormick et al.*, 1979, 1981]. SAM II views the Sun as it is occulted by the Earth's atmosphere; because of the near-polar orbit of Nimbus, SAM II only views the polar regions. Monthly mean polar stratospheric optical depths at $\lambda = 1$ μm are shown in Figure 3. Values near the peak optical depth after El Chichon have been corrected for instrument saturation, as suggested by *McCormick and Trepte* [1987], the maximum correction factors being 1.4 in the Antarctic in February 1983 and 2.0 in the Arctic in March 1983. (Instrument saturation is an even more serious problem with the greater optical depths for Pinatubo; an improved SAGE instrument proposed by McCormick for future satellite missions [*Hansen et al.*, 1992*b*] would be capable of measuring larger optical depths.) Thus the values in Figure 3 refer to the integrated optical depth down to the level 2 km above the tropopause. Annual winter maxima, evident especially in the Antarctic but also in the Arctic in recent years, are due to polar stratospheric clouds [*McCormick et al.*, 1982].

SAM II data are combined with low- and middle-latitude data to make the contour plot Figure 2*b* about the time of the El Chichon eruption. The optical depths in this figure (and others in this paper, with the exception of Figure 3) all refer to $\lambda = 0.55$ μm, where incoming solar energy peaks. SAM II data are converted to visible wavelengths by using the ratio of SAGE 1 μm and visible optical depths, or when SAGE is not available, by assuming a $1/\lambda$ dependence of optical depth on wavelength. For the period before SAGE II, low- and middle-latitude data were compiled from a variety of aircraft, ground-based and balloon observations by one of us (J. B. Pollack), including data from observations carried out in

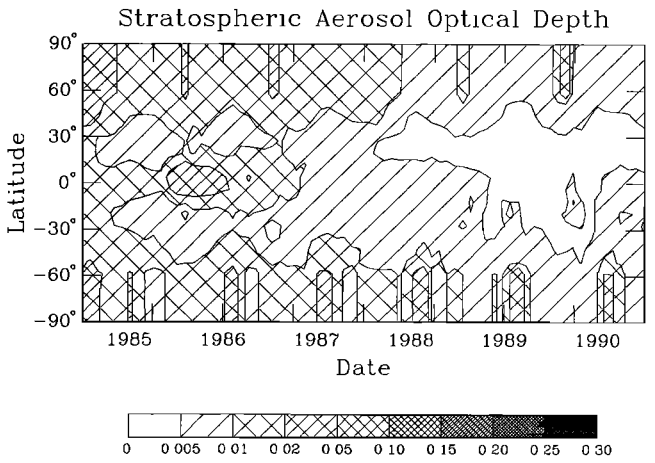

Fig. 4. Estimated stratospheric aerosol optical depth at $\lambda = 0.55$ μm as a function of latitude and time based on satellite measurements of SAM II and SAGE II. Observations are converted to wavelength 0.55 μm under the assumption that the optical depth varies inversely with the wavelength.

NASA field campaigns (e.g., see the special issues of *Geophysical Research Letters*, November, 1983, and *Geofisica Internacional*, April and July, 1984). SAM II optical depths at 1 μm and lidar integrated backscattering cross sections were scaled to optical depths at 0.55 μm by applying Mie scattering calculations to size distributions estimated from a combination of multispectral optical measurements and in situ size observations. The purpose of this procedure is to fit the data at available wavelengths, which are always limited, in a way which is physically consistent and allows extrapolation to all wavelengths. Note in Figure 2 that the El Chichon aerosols penetrated into the hemisphere opposite the eruption more effectively than the Agung aerosols, but the hemispheric mean optical depth was twice as large in the northern hemisphere as in the southern hemisphere.

Satellite measurements at lower latitudes are available from the Stratospheric Aerosol and Gas Experiment (SAGE) I and II [*McCormick and Wang*, 1987]. Both of these instruments were on spacecraft launched into orbits inclined about 55° to the Earth's equator, allowing observations between about 70°N and 70°S. SAGE I was on Atmospheric Explorer Mission B, launched in February 1979. It obtained sunrise and sunset occultation measurements for only 4 months, when partial failure of the spacecraft power system reduced observations to sunset events only; these were continued until the final failure of the satellite power system in November 1981. SAGE II, on the Earth Radiation Budget Satellite, began its observations in October 1984 and continues to function successfully.

SAM II and SAGE II data are combined in the latitude-time contour plot, Figure 4. Unfortunately, satellite data were not available at most latitudes for the El Chichon eruption, although that period was filled in with less detail by nonsatellite observations (Figure 2). Figure 4 illustrates the decay of the El Chichon aerosols and insertion and dispersal of aerosols from the Ruiz eruption in November 1985 and from a very small volcano (Kelut, 8°S) in February 1990.

Period after 1990. We initiated our GCM simulations [*Hansen et al.*, 1992*a*, 1993] soon after the eruption of Pinatubo (Philippines, 15°N, June 1991). Thus the aerosol properties we employed were crude estimates, based on the assumption that the optical depths following Pinatubo were about twice the values after El Chichon. These optical depths will be replaced in our on-line data set once a comprehensive analysis of observational data becomes available.

3. Discussion

Radiative forcing of the climate system by stratospheric aerosols depends primarily on the aerosol optical depth for solar radiation [*Lacis et al.*, 1992]. Specifically, Lacis et al. suggest that the net radiative flux change at the tropopause caused by addition of a globally uniform stratospheric aerosol layer can be approximated by

$$\Delta F_{\text{net}}\ (\text{W/m}^2) \sim 30\tau$$

where τ is the optical depth at $\lambda = 0.55$ μm, within an accuracy of about 25% for aerosol size distributions with effective radius [*Hansen and Travis*, 1974] between 0.1 and 1 μm.

The uncertainty in the estimated stratospheric aerosol optical depth is difficult to quantify, though it obviously tends to increase as we go farther back in time. For optical depth averaged over several years, we subjectively estimate typical errors as about 25% in the period 1915–1990, with a minimum uncertainty of 0.01, and about 50% in the period 1850–1915, again with a minimum uncertainty of 0.01. Although these uncertainties are large, we believe that the estimated history of aerosol optical depth provides a useful measure of volcanic aerosol climate forcing for the past century. Indeed, other than greenhouse gases, it may be the best known of the several suspected global climate forcings for that period [*Hansen et al.*, 1993].

This same comparison of climate forcings [*Hansen et al.*, 1993] implies that volcanic aerosols are one of the largest global climate forcings of the past century. Therefore it is important to improve the accuracy with which the volcanic climate forcing is specified, to the extent that is practical. For example, we note that one of the data sources mentioned above, lunar eclipse observations, have only been exploited for the period since 1960; it would be valuable for earlier eclipse data to be analyzed and published. For the future a considerably more precise measure of volcanic climate forcing could be obtained with an improved version of the SAGE satellite instrument [*Hansen et al.*, 1992*b*].

Comprehensive study of the climate response to large volcanic eruptions requires more information than the aerosol optical depth. Stratospheric heating, for example, depends strongly on the aerosol size and composition [*Lacis et al.*, 1992], and stratospheric temperature change may affect the distribution and magnitude of surface temperature response as well as the stratosphere itself [*Graf et al.*, 1992]. Our initial simulations for Pinatubo [*Hansen et al.*, 1992*a*] assumed that the effective particle size decreased during the 6 months following the eruption, as had been reported from limited in situ sampling after El Chichon [*Hofmann and Rosen*, 1983*a*, *b*]. Sampling after Agung yielded a similar temporal variation of sizes [*Mossop*, 1964]. But data for Pinatubo suggest an increasing effective radius with time [*Pueschel et al.*, 1992]. Because of variations in particle size with time, altitude, and geographic location it is highly desirable to monitor the particle size globally from space.

It also would be valuable to have an estimate of volcanic aerosol climate forcing on longer timescales. Perhaps the best proxy aerosol data are acidity of annual snow layers in the Greenland, Antarctic, and other ice sheets [e.g., *Hammer et al.*, 1980; *Legrand and Delmas*, 1987]. It may be useful to calibrate the acidity data against the optical depths we have derived for the past century, thus allowing the acidity data to be used in climate simulations for periods such as the past several hundred years, which are also of great interest. However, it would be necessary to use data from ice cores at several places on the planet to isolate the influence of local sources.

Our objective has been to put together a stratospheric aerosol index which can be used for simulations of climate of the past 140 years. Although this aerosol forcing is not as accurate as the greenhouse gas forcing for the same period, it would appear to be better to employ it in studies such as global climate sensitivity than to neglect stratospheric aerosol forcing altogether. The data set is available from the authors, and we welcome information on existing observational data or other suggestions which would improve future versions of the data set. The data access procedure is (1) FTP NASAGISS.GISS.NASA.GOV, (2) log on as ANONYMOUS, (3) give your last name as password, (4) GET STRAT.HELP, (5) GET STRAT.AEROSOLS, (6) quit to log off.

Acknowledgments. We thank Mary Osborn, Michael Pitts, Jean Lerner, and Richard Stothers for help with data and scientific discussions and Jeffrey Jonas for assistance with graphics.

REFERENCES

Angell, J. K., and J. Korshover, Surface temperature changes following six major volcanic episodes between 1780 and 1980, *J. Clim. Appl. Meteorol.*, *24*, 937–951, 1985.

Coakley, J. A., and G. W. Grams, Relative influence of visible and infrared optical properties of a stratospheric aerosol layer on the global climate, *J. Appl. Meteorol.*, *15*, 679–691, 1976.

Dutton, E. J., and J. R. Christy, Solar radiative forcing at selected locations and evidence for global lower tropospheric cooling following the eruptions of El Chichon and Pinatubo, *Geophys. Res. Lett.*, *19*, 2313–2316, 1992.

Dyer, A. J., The effect of volcanic eruptions on global turbidity and an attempt to detect long-term trends due to man, *Q. J. R. Meteorol. Soc.*, *100*, 563–571, 1974.

Dyer, A. J., and B. B. Hicks, Global spread of volcanic dust from the Bali eruption of 1963, *Q. J. R. Meteorol. Soc.*, *94*, 545–554, 1968.

Graf, H. F., I. Kirchner, A. Robock, and I. Schult, Pinatubo eruption winter climate effects: Model versus observations, *Tech. Rep. 94*, 24 pp., Max-Planck-Inst. für Meteorol., Hamburg, 1992.

Hammer, C. U., H. B. Clausen, and W. Dansgaard, Greenland ice sheet evidence of post-glacial volcanism and its climatic impact, *Nature*, *288*, 230–235, 1980.

Hansen, J. E., and A. A. Lacis, Sun and dust versus greenhouse gases: An assessment of their relative roles in global climate change, *Nature*, *346*, 713–719, 1990.

Hansen, J. E., and S. Matsushima, Light illuminance and color in the Earth's shadow, *J. Geophys. Res.*, *71*, 1073–1081, 1966.

Hansen, J. E., and L. D. Travis, Light scattering in planetary atmospheres, *Space Sci. Rev.*, *16*, 527–610, 1974.

Hansen, J. E., W. C. Wang, and A. A. Lacis, Mount Agung eruption provides test of a global climate perturbation, *Science*, *199*, 1065–1068, 1978.

Hansen, J. E., A. A. Lacis, P. Lee, and W. C. Wang, Climatic effects of atmospheric aerosols, *Ann. N. Y. Acad. Sci.*, *338*, 575–587, 1980.

Hansen, J., A. Lacis, R. Ruedy, and M. Sato, Potential climate impact of Mount Pinatubo eruption, *Geophys. Res. Lett.*, *19*, 215–218, 1992*a*.

Hansen, J., W. Rossow, and I. Fung, Long-term monitoring of global climate forcings and feedbacks, *NASA Conf. Publ.*, 89 pp., New York, 1992*b*.

Hansen, J., A. Lacis, R. Ruedy, M. Sato, and H. Wilson, How sensitive is the world's climate?, *Res. Explor.*, *9*, 142–158, 1993.

Harshvardhan, and R. D. Cess, Stratospheric aerosols: Effect upon atmospheric temperature and global climate, *Tellus*, *28*, 1–10, 1976.

Hofmann, D. J., and J. M. Rosen, Sulfuric acid droplet formation and growth in the stratosphere after the 1982 eruption of El Chichon, *Science*, *222*, 325–327, 1983*a*.

Hofmann, D. J., and J. M. Rosen, Stratospheric sulfuric acid fraction and mass estimates for the 1982 volcanic eruption of El Chichon, *Geophys. Res. Lett.*, *10*, 313–316, 1983*b*.

Hoyt, D. V., An explosive volcanic eruption in the southern hemisphere in 1928, *Nature*, *275*, 630–632, 1978.

Hoyt, D. V., Pyrheliometric and circumsolar sky radiation measurements by the Smithsonian Astrophysical Observatory from 1923 to 1954, *Tellus*, *31*, 217–229, 1979*a*.

Hoyt, D. V., Atmospheric transmission from the Smithsonian Astrophysical Observatory pyrheliometric measurements from 1923 to 1957, *J. Geophys. Res.*, *84*, 5018–5028, 1979*b*.

Hoyt, D., and C. Frohlich, Atmospheric transmission data at Davos, Switzerland, 1909–1979, *Clim. Change*, *5*, 61–71, 1983.

Keen, R. A., Volcanic aerosols and lunar eclipses, *Science*, *222*, 1011–1013, 1983.

Kelly, P. M., and C. B. Sear, Climatic impact of explosive volcanic eruptions, *Nature*, *311*, 740–743, 1984.

Kimball, H. H., Variation in solar radiation intensities measured at the surface of the Earth, *Mon. Weather Rev.*, *52*, 527–529, 1924.

Lacis, A., J. Hansen, and M. Sato, Climate forcing by stratospheric aerosols, *Geophys. Res. Lett.*, *19*, 1607–1610, 1992.

Lamb, H. H., Volcanic dust in the atmosphere, with a chronology and assessment of its meteorological significance, *Phil. Trans. R. Soc. London, Ser. A*, *266*, 425–533, 1970.

Legrand, M., and R. J. Delmas, A 220-year continuous record of volcanic H_2SO_4 in the Antarctic ice sheet, *Nature*, *327*, 671–676, 1987.

Link, F., Eclipse phenomena, *Adv. Astron. Astrophys.*, *2*, 87–198, 1963.

Lockwood, G. W., and D. T. Thompson, Atmospheric extinction: The ordinary and volcanically induced variations, 1972–1985, *Astron. J.*, *92*, 976–985, 1986.

Mass, C. F., and D. A. Portman, Major volcanic eruptions and climate: A critical evaluation, *J. Clim.*, *2*, 566–593, 1989.

Mass, C. F., and S. H. Schneider, Statistical evidence of the influence of sunspots and volcanic dust on long term temperature records, *J. Atmos. Sci.*, *19*, 2313–2316, 1977.

McCormick, M. P., and C. R. Trepte, Polar stratospheric optical depth observed between 1978 and 1985, *J. Geophys. Res.*, *92*, 4297–4306, 1987.

McCormick, M. P., and P. H. Wang, Satellite measurements of stratospheric aerosols, in *Transport Processes in the Middle Atmosphere*, edited by G. Visconti and R. Garcia, pp. 103–120, D. Reidel, Norwell, Mass., 1987.

McCormick, M. P., P. Hamill, T. J. Pepin, W. P. Chu, T. J. Swissler, and L. R. McMaster, Satellite studies of the stratospheric aerosol, *Bull. Am. Meteorol. Soc.*, *60*, 1038–1046, 1979.

McCormick, M. P., W. P. Chu, G. W. Grams, P. Hamill, B. W. Herman, L. R. McMaster, T. J. Pepin, P. B. Russell, H. M. Steele, and T. J. Swissler, High-latitude stratospheric aerosols measured by the SAM II satellite system in 1978 and 1979, *Science*, *214*, 328–331, 1981.

McCormick, M. P., H. M. Steele, P. Hamill, W. P. Chu, and T. J. Swissler, Polar stratospheric cloud sightings by SAM II, *J. Atmos. Sci.*, *39*, 1387–1397, 1982.

Mitchell, J. M., A preliminary evaluation of atmospheric pollution as a cause of the global temperature fluctuation of the past century, in *Global Effects of Environmental Pollution*, edited by S. F. Singer, pp. 139–155, Springer-Verlag, New York, 1970.

Mossop, S. C., Volcanic dust collected at an altitude of 20 km, *Nature*, *203*, 824–827, 1964.

Newhall, C. G., and S. Self, The volcanic explosivity index (VEI):

An estimate of explosive magnitude for historical volcanism, *J. Geophys. Res.*, *87*, 1231–1238, 1982.

Pollack, J. B., O. B. Toon, C. Sagan, A. Summers, B. Baldwin, and W. Van Camp, Stratospheric aerosols and climatic change, *Nature*, *263*, 551–555, 1976*a*.

Pollack, J. B., O. B. Toon, C. Sagan, A. Summers, B. Baldwin, and W. Van Camp, Volcanic explosions and climatic change: A theoretical assessment, *J. Geophys. Res.*, *81*, 1071–1083, 1976*b*.

Pueschel, R. F., S. A. Kinne, P. B. Russell, K. G. Snetsinger, and J. M. Livingston, Effects of the 1991 Pinatubo volcanic eruption on the physical and optical properties of stratospheric aerosols, in *IRS '92: Current Problems in Atmospheric Radiation*, edited by S. Keevallik, pp. 183–186, A. Deepak, Hampton, Va., 1992.

Rampino, M. R., S. Self, and R. B. Stothers, Volcanic winters, *Ann. Rev. Earth Planet. Sci.*, *16*, 73–99, 1988.

Robock, A., A latitudinally dependent volcanic dust veil index, and its effect on climate simulations, *J. Volcanol. Geotherm. Res.*, *11*, 67–80, 1981.

Robock, A., The volcanic contribution to climate change of the past 100 years, in *Greenhouse-Gas-Induced Climatic Change: A Critical Appraisal of Simulations and Observations*, edited by M. E. Schlesinger, pp. 429–443, Elsevier, New York, 1991.

Sapper, K., *Vulkankunde*, 424 pp., Engelhorn Verlag, Stuttgart, Germany, 1927.

Self, S., and M. R. Rampino, The relationship between volcanic eruptions and climate change: Still a conundrum? *Eos Trans. AGU*, *69*, 74–75, 85–86, 1988.

Simkin, T., L. Siebert, L. McClelland, D. Bridge, C. Newhall, and J. H. Latter, *Volcanoes of the World*, 232 pp., Hutchinson Ross, Stroudsburg, Pa., 1981.

Stommel, H., and E. Stommel, *Volcano Weather*, 177 pp., Seven Seas Press, Newport, R. I., 1983.

Stothers, R., The great Tambora eruption in 1815 and its aftermath, *Science*, *224*, 1191–1198, 1984.

Thompson, L. G., and E. Mosley-Thompson, Temporal variability of microparticle properties in polar ice sheets, *J. Volcanol. Geotherm. Res.*, *11*, 11–27, 1981.

Toon, O. B., Climatic change on the Earth and Mars, Ph.D. thesis, Cornell Univ., Ithaca, N. Y., 1975.

J. E. Hansen and M. Sato, NASA Goddard Institute for Space Studies, 2880 Broadway, New York, NY 10025.

M. P. McCormick, NASA Langley Research Center, Hampton, VA 23665.

J. B. Pollack, NASA Ames Research Center, Moffett Field, CA 94035.

(Received March 30, 1993;
revised July 21, 1993;
accepted September 7, 1993.)